Structural Determinants of High-Affinity Binding of Ryanoids to the Vertebrate Skeletal Muscle Ryanodine Receptor: A Comparative Molecular Field Analysis†

William Welch,*,‡ Syed Ahmad,§ Judith A. Airey,§ Koert Gerzon,‖ Rod A. Humerickhouse,‖ Henry R. Besch, Jr.,‖ Luc Ruest,⊥ Pierre Deslongchamps,⊥ and John L. Sutko§

Departments of Biochemistry and Pharmacology, University of Nevada, Reno, Nevada 89557, Department of Pharmacology and Toxicology, Indiana University, Indianapolis, Indiana 43223, and Laboratoire de Synthèse Organique, Département de Chimie, Faculté des Sciences, Université de Sherbrooke, Sherbrooke, Québec, Canada J1K 2R1

Received November 3, 1993; Revised Manuscript Received February 21, 1994®

ABSTRACT: Ryanodine binds to specific membrane proteins, altering the calcium permeability of intracellular membranes. In this study 19 ryanoids were isolated or synthesized and the structures correlated to the strength of binding to vertebrate skeletal muscle ryanodine receptors. Global minima were determined by employment of molecular mechanics and dynamics augmented by systematic searching of conformational space. Overall, steric and electrostatic factors contribute about equally to the differences in the experimentally determined dissociation constants. The dominant electrostatic interaction is localized to a hydroxyl group in an apolar region of the molecule. The pyrrole and isopropyl groups located together at one pole of the molecule have the greatest effect on steric interactions between ligand and receptor. We suggest ryanodine binds to the receptor with the pyrrole and isopropyl groups buried deep inside a cleft in the protein. This arrangement places special importance on the conformation of the pyrrole and isopropyl groups. In contrast, the opposite pole appears to be positioned at the entrance of the binding pocket because bulky adducts placed in the 9 position of ryanodine alter binding minimally. For example, a fluorescent ryanodine adduct was synthesized which has a dissociation constant close to that of ryanodine. Detailed examination reveals subtle interactions between ryanoid and receptor. In many cases, the major factors altering the strength of binding were found to be conformational alterations in the molecule remote from the site of covalent modification.

The plant alkaloid ryanodine (**1**, Scheme 1), a natural insecticide (DeVault, 1983), was isolated originally from the wood of *Ryania speciosa* Vahl (Rogers *et al.*, 1948). Studies of the effects of ryanodine on invertebrates and vertebrates revealed powerful actions on the contraction of striated muscle (Jenden & Fairhurst, 1969). The mechanistic basis of the actions of this agent on vertebrate skeletal muscle was shown to involve effects on the calcium permeability of sarcoplasmic reticulum (SR) by Fairhurst and his colleagues (Fairhurst & Hasselbach, 1970; Fairhurst, 1974). Similar actions were demonstrated for cardiac muscle (Hillyard & Procita, 1959; Nayler *et al.*, 1970; Penefsky & Kahn, 1970; Penefsky, 1974; Frank & Sleator, 1975; Sutko *et al.*, 1979; Jones *et al.*, 1979; Jones & Cala, 1981; Hilgemann *et al.*, 1983). Subsequent studies demonstrated that ryanodine is a specific effector of SR calcium release that can increase, as well as decrease, SR membrane calcium permeability (Fleischer *et al.*, 1985; Meissner, 1986; Lattanzio *et al.*, 1987). Ryanodine was tritiated to a high specific activity (Fairhurst, 1971; Waterhouse *et al.*, 1984; Sutko *et al.*, 1986; Inui *et al.*, 1987) and demonstrated to be a specific ligand for the triad junctional foot protein, now commonly referred to as the ryanodine receptor (Pessah *et al.*, 1986; Inui *et al.*, 1987; Campbell *et al.*, 1987; Lai *et al.*, 1988). The criterion of specific [^{3}H]-ryanodine binding was used to purify, clone, and functionally express the receptor protein (Takeshima *et al.*, 1989; Zorzato *et al.*, 1990).

[^{3}H]Ryanodine binds to its receptor in a complex manner, displaying multiple affinities and cooperative binding (Lai *et al.*, 1989; Chu *et al.*, 1990; Pessah & Zimanyi, 1991; Carroll *et al.*, 1991b). Ryanodine binding alters the conductance properties of the ryanodine receptor calcium channel in an intricate manner. Submicromolar concentrations of this agent increase the open probability of this channel, locking it in a long-lived open state, whereas micromolar or greater concentrations inhibit this conductance (Rousseau *et al.*, 1987; Smith *et al.*, 1988). Moreover, multiple conductance states have been observed for the channel (Liu *et al.*, 1989).

Given the complicated interactions between ryanodine and its receptor, it becomes of interest to identify the structural aspects of the ryanodine molecule that are essential for these phenomena. Waterhouse *et al.* (1987) and Jefferies *et al.* (1993) have described the relative potency of a variety of ryanodine derivatives as ligands for the high-affinity ryanodine binding site. We have employed computational techniques to quantify attributes of the ryanodine molecule important for binding to the triad junctional foot protein or ryanodine receptor (RyR). In these studies we utilized a number of naturally occurring ryanodine congeners identified and characterized by Ruest *et al.* (1985) in combination with some previously unreported ryanodine derivatives. For this task we have taken advantage of developments of quantitative structure–function analysis (QSAR) including comparative molecular field analysis (CoMFA), which was introduced by Cramer *et al.* (1988). In the CoMFA technique the steric (Lennard-Jones) and electrostatic (Coulombic) fields are calculated at discrete points in the space surrounding each molecule in a basis set of molecules. The changes in steric and electrostatic values at each point are then correlated with

† Supported by a Glaxo Cardiovascular Discovery Grant, the National Institutes of Health (HL27470), the American Heart Association, the Showalter Trust, and the University of Nevada Molecular Modeling/Graphics Facility.

* Corresponding author.
‡ Department of Biochemistry, University of Nevada.
§ Department of Pharmacology, University of Nevada.
‖ Indiana University.
⊥ Université de Sherbrooke.

® Abstract published in *Advance ACS Abstracts,* May 1, 1994.

0006-2960/94/0433-6074$04.50/0

measured changes in biological properties. Past reports have demonstrated the predictive ability of this technique [*e.g.*, Marshall and Cramer (1988), Clark (1990), Maret *et al.* (1990), Silipo and Vittoria (1991), Kim and Martin (1991a,b), Allen *et al.* (1990), and Carroll *et al.* (1991a)]. In the present study, we identify correlations between the structures of ryanodine and 18 of its congeners and analogs with the binding affinities of these compounds for the ryanodine receptors present in chicken and rabbit skeletal muscles.

MATERIALS AND METHODS

Calculations were performed on an Evans and Sutherland ESV50 and PS390 and a Sun 4 using SYBYL versions 5.32–6.0 (Tripos Associates, St. Louis, MO). Unless stated otherwise, atomic charges were estimated by the method of Gasteiger and Marsili (Gasteiger & Marsili, 1980, 1981; Marsili & Gasteiger, 1980).

Definition of Torsional Angles. An initial CoMFA indicated that the conformation of the isopropyl and pyrrole groups is an important determinant of binding. Therefore, the movement of the pyrrole ring was approximated by measuring the torsional angles (torsion 1, 2, 3) of the three rotatable bonds connecting the pyrrole ring to the main body (polycyclic ring system) of the ryanodine analogs. The motion of the isopropyl group was followed by the torsion (torsion 4) of the single bond connecting the ring system to the propyl group. The angles are defined by looking toward the polycyclic ring system: torsion 1, atoms 24, 25, 23, 35; torsion 2, atoms 35, 23, 22, 3; torsion 3, atoms 23, 22, 3, 2; torsion 4, atoms 18, 13, 2, 1 (see Figure 1 for the numbering system).

Global Energy Minima. Multiple methods were used to ensure the global minimum of each molecule was found: (a) Minimum energy conformations were calculated using molecular mechanics with a variety of convergence algorithms. The BFGS, conjugate gradient (Press *et al.*, 1988), and Powell (1977) methods were used with equivalent results. (b) The ryanoids were submitted to molecular dynamics (MD) at 310 K for 10 ps of simulation time. From the resulting conformational databases, conformations sampled at the extrema of simulation time, potential energies, and radii of gyration were minimized by molecular mechanics. (c) To explore a wider range of conformations, ryanoids were submitted to simulated annealing through a heating and cooling cycle essentially as described by Homans (1990). (d) Further exploration of conformational space was accomplished by using a "grid search" or "dihedral driver" algorithm (Burkert & Allinger, 1982). The lowest energy conformation of each molecule found by the application of all of these methods (a–d) was taken as the global minimum. A dielectric constant of one was used except where noted. The conformational minimum of ryanodine was also calculated using the procedures described above with water included explicitly in the calculations as solvent. The positions of the non-hydrogen atoms were the same for the *in vacuo* and solvent calculations. Therefore, water was not included in any other calculations described in this report.

Semiempirical Quantum Mechanics. Conformations and atomic charges were calculated using semiempirical quantum mechanics using the MOPAC suite of Hamiltonians as included in the SYBYL package. For the present studies, only the geometry optimization and heat of formation calculations were used to aid in the assignment of ryanoid conformation. Calculated charges and molecular orbitals will be included in the analysis in the future. None of the present calculations were inconsistent with those predicted by molecular mechanics.

Estimation of Hydrophobic Interactions. The program HINT (Kellogg *et al.*, 1991) was used to estimate the strength of hydrophobic interactions. This program is based on data of Hansch and co-workers [*e.g.*, Hansch and Leo (1979)]. To test the use of HINT in our application, we examined some compounds whose properties were known. Whereas the differences in hydrophobic free energies derived from the values of log *P* estimated by HINT (unified atom method) were in excellent agreement with published values for most compounds [*e.g.*, Kauzmann (1959)], the results obtained for pyrroles were not as successful. Dr. Kellogg (personal communication) suggested that the atom type assigned by SYBYL to the pyrrole nitrogen be changed to aromatic and hydrogens be explicitly included in the calculations. Using this method the values of log *P* were in good agreement with the experimental values for pyrrole and pyridine. Therefore, the differences in hydrophobicity between the ryanoids were calculated using this suggestion. Both the bond and space methods were used for the ryanoid calculations. When the two methods gave divergent estimates, a range of values is reported.

Estimation of the Contribution of Specific Structural Loci. The predict function of the CoMFA was used to estimate the contribution of specific regions of individual ryanoids to the observed variation in dissociation constant. For example, to calculate the importance of electrostatic interactions, all charges on a particular ryanoid were set to zero. The predict function was used to calculate the natural logarithm of the dissociation constant of the hypothetical compound. The predicted value of a hypothetical ryanodine molecule whose atomic charges had been removed was subtracted from this value. The calculated difference was then compared to the difference between the natural logarithms of the dissociation constants of the unmodified ryanoid and ryanodine. If the difference between the hypothetical pair was zero, then electrostatic contributions alone accounted for the difference in binding of the real compounds. On the other hand, if the differences between the hypothetical pair and the "real" pair were identical, then electrostatic differences contributed nothing to the observed difference in binding. The values were normalized by dividing the difference between hypothetical compounds by the difference between the real compounds. To estimate the contribution of a particular locus to the difference in binding, an analogous calculation was performed. For example, to estimate the contribution of the pyrrole locus, the exocyclic substituents at position 3 were removed without altering either the geometry or atomic charges on the remainder of the molecule.

The strategy outlined above can be applied generally. Let X be $\ln(K_D)$ of a ryanoid and X' be the predicted $\ln(K_D)$ of a hypothetical ryanoid. Let Y be the $\ln(K_D)$ of ryanodine and Y' the $\ln(K_D)$ of the hypothetical ryanodine with the same modifications as X'. Then the fraction contribution of a modification (f) is $f = [(X - Y) - (X' - Y')]/(X - Y) = 1 - [(X' - Y')/(X - Y)]$. The hypothetical compounds could include those formed by removal of charge or exocyclic substituents as illustrated above. To estimate the contribution of changes in the polycyclic ring system, the equation becomes $f = (X' - Y')/(X - Y)$, where X' and Y' are the predicted $\ln(K_D)$ of hypothetical ryanoids with all of the modified exocyclic substituents removed.

[^{3}H]Ryanodine Binding Assay. The relative affinities of the ryanodine congeners and derivatives for the ehicken and rabbit skeletal muscle ryanodine receptors were determined in competitive binding assays. Ligand binding was measured at 37 °C in a 200-μL final volume containing 0.5 M KCl, 20

Scheme 1: Natural Ryanoids from *Ryania speciosa* Vahl

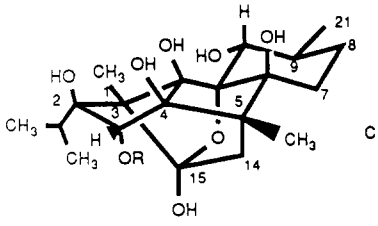

1: Ryanodine

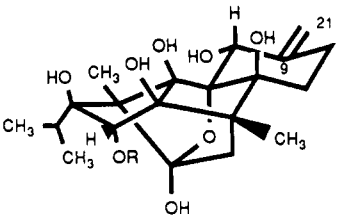

2 : Dehydroryanodine

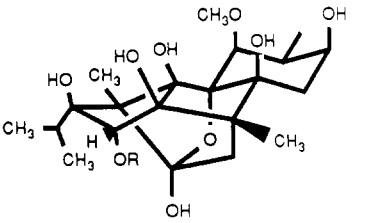

3 : Ester A

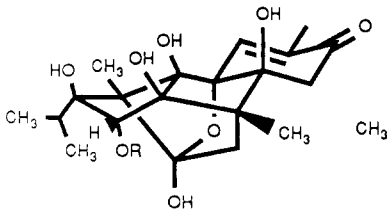

4 : Ester B

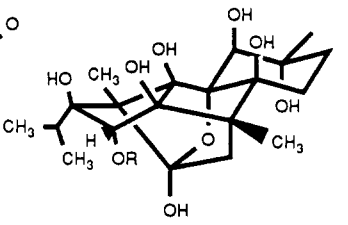

5 : Ester C_1

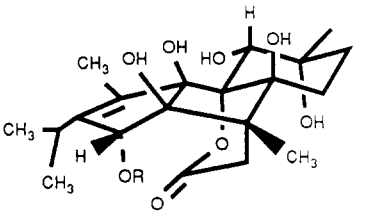

6 : Ester C_2

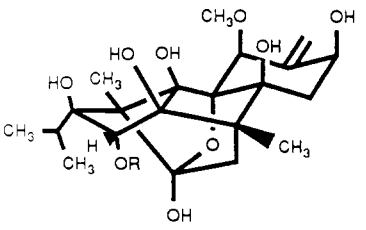

7 : Ester D

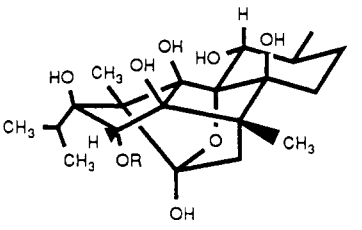

8: R= 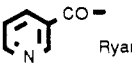 Ryanodyl nicotinate

9: R= H: Ryanodol

R= 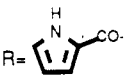 , unless otherwise indicated

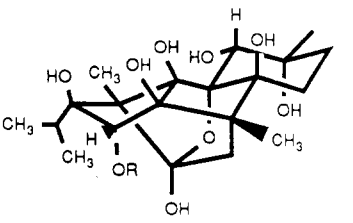

10: 9-Hydroxyryanodine

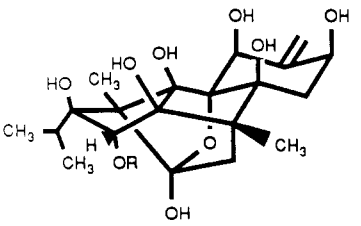

11: 10-O-Desmethyl-ester D

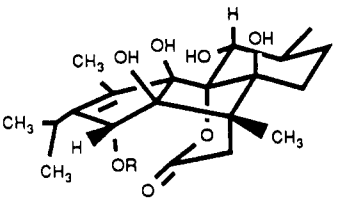

12: Anhydroryanodine

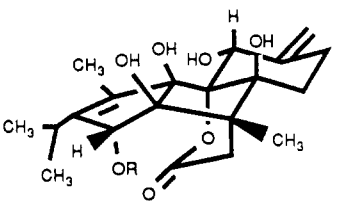

13: 9,21-Didehydroanhydroryanodine

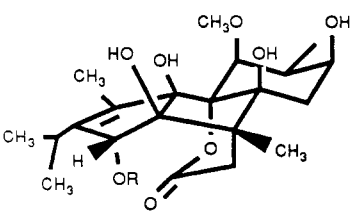

14 : Anhydroester A

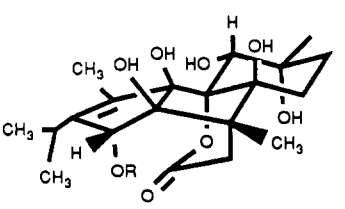

15: 9-Hydroxyanhydroryanodine

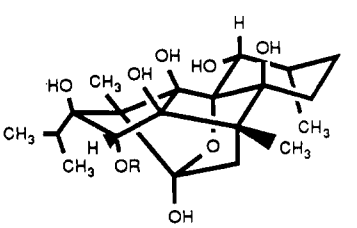

16: 9-Epiryanodine

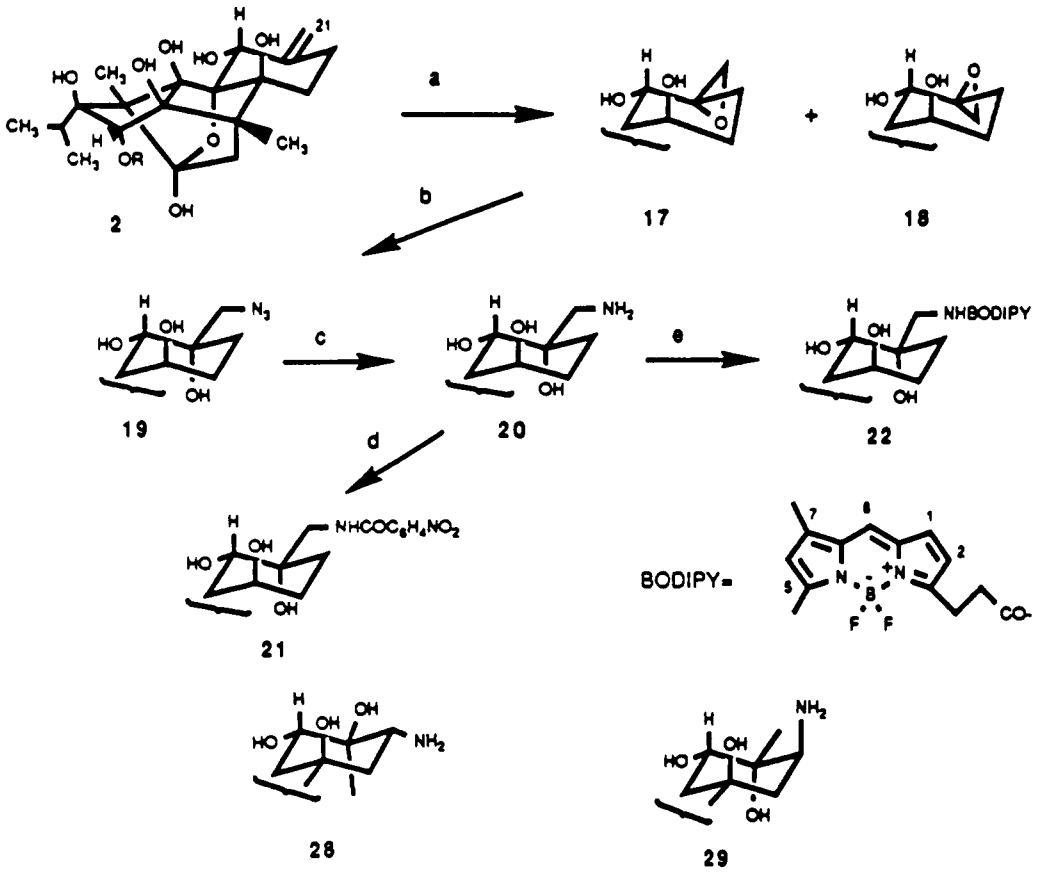

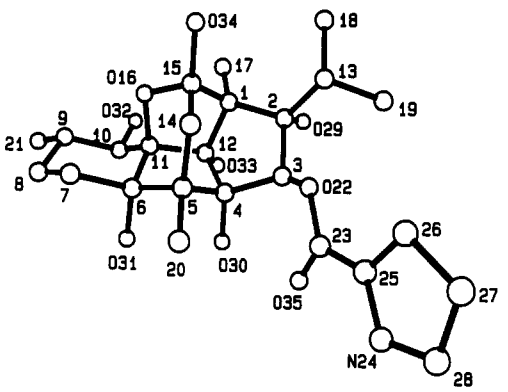

FIGURE 1: Ball and stick model of ryanodine. The heavy atoms of ryanodine are shown in this perspective drawing to illustrate the global minimum conformation as well as the numbering system used in this paper. Oxygen atoms are indicated by the prefix O and nitrogen atoms by the prefix N.

mM Tris, pH 7.4, 200 μM $CaCl_2$, 2.5 mM AMP, and 6.7 nM [^{3}H]ryanodine (Sutko *et al.*, 1986). Concentrations of the ryanoid to be tested ranged from 0.1 nM to 30 μM. Nonspecific binding was assessed in the presence of 10 μM nonlabeled ryanodine. Binding reactions were initiated by the addition of 40 μg of muscle microsomal protein and terminated 2 h later by collection of the membranes onto Whatman GF/B glass fiber filters and washing four times with 4-mL aliquots of an ice-cold solution containing 0.5 M KCl, 20 mM Tris, pH 7.4, and 200 μM $CaCl_2$. The radioactivity retained by the filters was measured in a liquid scintillation counter. Skeletal muscle microsomal membranes were prepared as described previously (Airey *et al.*, 1990) and exhibited 3–5 pmol/mg protein of specific [^{3}H]ryanodine binding. Results represent averages of at least three different determinations. Apparent dissociation constants were calculated using the relation $K_C = K_D[C]/(K_D + [R])$, where K_C is the dissociation constant of the ryanoid under consideration, K_D is the dissociation constant of ryanodine (measured in a direct binding assay), [C] is the concentration of the ryanoid required to displace one-half of the bound [^{3}H]-ryanodine, and [R] is the fixed concentration of ryanodine used in the competition assays.

RESULTS

In this section we will describe (1) the construction of the basis set of ryanoids used for the volume analysis and the CoMFA, (2) the general properties found to correlate with binding of the ryanoids to vertebrate skeletal muscle ryanodine receptors, and (3) the results of a close examination of selected members of the basis set.

(1) Construction of the Basis Set

The conformation corresponding to the global energy minimum of each ryanoid was used as the basis of comparison. The molecules are listed in Table 1 and the structural formulas presented in Scheme 1. The numbering system used in this paper is illustrated in Figure 1, which is a ball and stick representation of ryanodine in the conformation corresponding to the global minimum. For clarity, hydrogen atoms have been omitted from this figure. The heteroatoms are indicated by the prefixes N and O. The most prominent substituents are the pyrrole ring (atoms 24–28) and the isopropyl group (atoms 13, 18, 19). The pyrrole ring is linked to a polycyclic ring system via a formyl group (atoms 22, 23, 35). The ring system is substituted with methyl groups at positions 1, 5, and 9 and hydroxyl groups at positions 2, 4, 6, 10, 12, and 15. The orientation of the substituents is illustrated in Figure 2 in which the hydrophobic and polar fields are visualized. The hydroxyl groups are clustered and altogether occupy slightly more than one hemisphere of the molecule; the asymmetric

Table 1: Nomenclature and K_D for Ryanodine Analogs

reference no.	name used in this paper	name as a ryanodine derivative	K_D (nM) rabbit	K_D (nM) chicken
1	raynodine	ryanodine	7	7
2	dehydroryanodine	$\Delta^{9,21}$-ryanodine or 9,21-didehydroryanodine	7	6
3	ester A	8β-hydroxy-10-*O*-methyl-10-epiryanodine	110	130
4	ester B	$\Delta^{9,10}$-8-ketodes(10-hydroxy)ryanodine	240	240
5	ester C_1	9α-hydroxy-10-epiryanodine	210	300
6	ester C_2	$\Delta^{1,2}$-9α-hydroxyryanodine 15,16,11-lactone	2600	3600
7	ester D	$\Delta^{9,21}$-8β-hydroxy-10-*O*-methyl-10-epiryanodine	51	63
8	ryanodyl nicotinate	3-*O*-(pyridyl-3-carbonyl)ryanodol	1100	1400
9	ryanodol	3-*O*-des(pyrrolyl-2-carbonyl)ryanodine	12000	3600
10	9-hydroxyryanodine	9α-hydroxyryanodine	110	110
12	anhydroryanodine	$\Delta^{1,2}$-ryanodine 15,16,11-lactone	2900	3000
14	anhydroester A	8β-hydroxy-10-*O*-methyl-$\Delta^{1,2}$-10-epiryanodine 15,16,11-lactone	5200	8100
16	9-epiryanodine	9-epiryanodine	13	13
18	9β,21-epoxyryanodine	9β,21-epoxyryanodine	36	29
19	21-azido-9-hydroxyryranodine	21-azido-9α-hydroxyryanodine	78	87
21	(*p*-nitrobenzoyl)ryanodine	21-(*p*-nitrobenzamido)-9α-hydroxyryanodine	22	22
22	21-BODIPY-ryanodine	21-BODIPY-9α-hydroxyryanodine	13	13
28	8α,9β-dihydroxyryanodine	8α-amino-9β-hydroxyryanodine	3800	3800
29	8β,9α-dihydroxyryanodine	8β-amino-9α-hydroxyryanodine	760	760

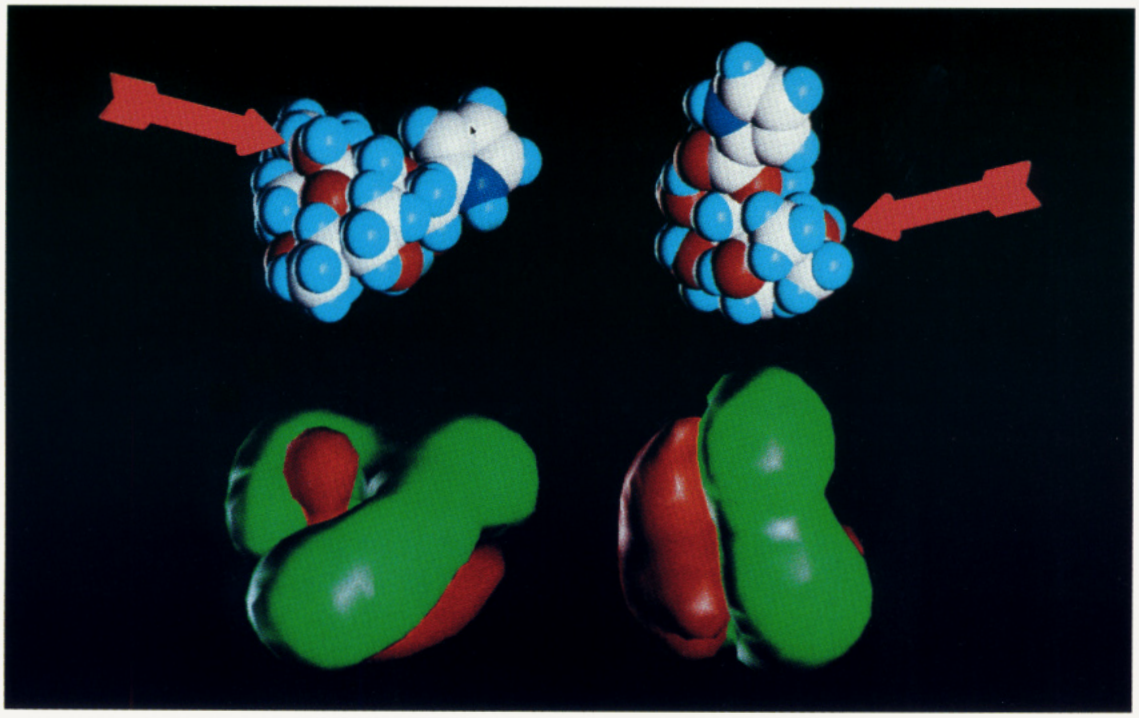

FIGURE 2: Visualization of the physical properties of ryanodine. The hydrophobic (green) and polar (red) fields surrounding ryanodine are shown. A space-filling model is shown above each field for orientation. The red arrow indicates the position of the hydroxyl group (O34) attached to position 15 (see text).

distribution makes the character of the two sides of ryanodine quite different. One hydroxyl group (at position 15, indicated by the red arrow) is somewhat apart from the others. As shown below, electrostatic forces at this position are highly correlated with ligand binding.

Motion of Pyrrole and Isopropyl Groups. The selection of the appropriate conformation for each member of the basis set received particular attention since preliminary analyses indicated that the isopropyl and the pyrrole groups were important determinants of ryanoid affinity. The position of these groups can be approximated by measuring the torsional angles of the bonds which connect them to the relatively rigid polycyclic ring system. The ryanoids are good candidates for modeling because there are few rotatable bonds and the motional freedom of the isopropyl and the pyrrole groups is quite restricted. To illustrate this, the motion of the atoms used to define the torsional angles (see Materials and Methods) is shown in Figure 3. At 37 °C the atoms are restricted to positions near the global minimum and in no case make a full rotation. A plot of the observed torsional angles is shown in Figure 4. Note that the torsional angles oscillate many times during the 10-ps observation period, indicating good equilibrium. The average torsional angles and the standard deviations of two ryanoids are shown in square brackets in Table 2. A more complete version of this table is deposited with this journal as supplementary material and is available from the corresponding author.

To map the conformational space of the ryanoids, the energy minima and rotational energy barriers of the bonds connecting the pyrrole and isopropyl to the polycyclic ring system were determined by a grid search (dihedral driver) algorithm as described above in Materials and Methods. Some of the results are listed in Table 2. The conformational minima found by the grid search of each molecule are compared to the values

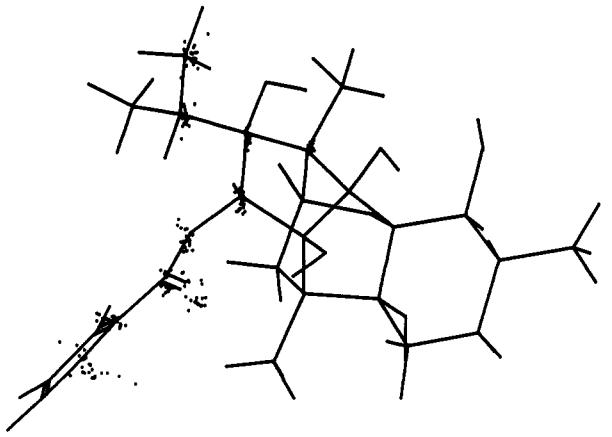

FIGURE 3: Motion of ryanodine. This figure illustrates the results of a molecular dynamics simulation of the motion of ryanodine at 37 °C. Ryanodine was equilibrated at 37 °C for 10 ps and then data were collected for an additional 20 ps. The dots show the position of the respective atoms at 1-ps intervals.

of the torsional angles found at the global minimum of that molecule. The small differences in torsional angles between closely related molecules at their respective global minima, *e.g.*, ryanodine and dehydroryanodine (supplementary material), were verified by semiempirical quantum mechanics from the MOPAC suite (AM1, MNDO, PM3).

Orientation of the Pyrrole Group. Because the motion of the pyrrole group is restricted and will not reorient at physiological temperatures, discrete conformers of the ryanoids exist. In this section the rationale for selecting one conformer for the basis set used in this paper is presented. Conformational searching identified definite minima for rotatable bonds 2–4 but indicated two minima of nearly equal energy for rotatable bond 1 (Table 2; see Materials and Methods and Figure 1 for the definition of the bonds). We have termed the two conformers *anti* (shown in Figures 1 and 2) and *syn*. In the *syn* conformer, the nitrogen atom of the pyrrole is directed toward the main bulk of the molecule (usually pointing toward the isopropyl group) and is on the side of ryanodine opposite from the large cluster of hydroxyl groups (Figure 2). Note that this definition is different from that used by Kaye *et al.* (1980) for other pyrrole-2-carboxylates but it is more appropriate for the ryanoids as it describes the position of the pyrrole in relation to the polycyclic ring system. The *anti* conformer (in which the pyrrole nitrogen is on the same side as the large cluster of hydroxyl groups) was used in this study.

The validity of the choice of the *anti* conformer as the global minimum was assessed by three methods. (1) Conformational searching indicated that the *anti* conformer had slightly more favorable strain energy. (2) Repeated simulated annealing produced the *anti* conformer. (3) Semiempirical quantum mechanical energy calculations (AM1 with full-geometry optimization) produced a heat of formation favoring the *anti* conformer. In addition to the calculated data, published experimental data for analogous compounds are consistent with the choice of the *anti* conformer. For example, Kaye *et al.* (1980) determined experimentally a 1.2 kcal/mol difference between the two orientations of the pyrrole of *tert*-butyl

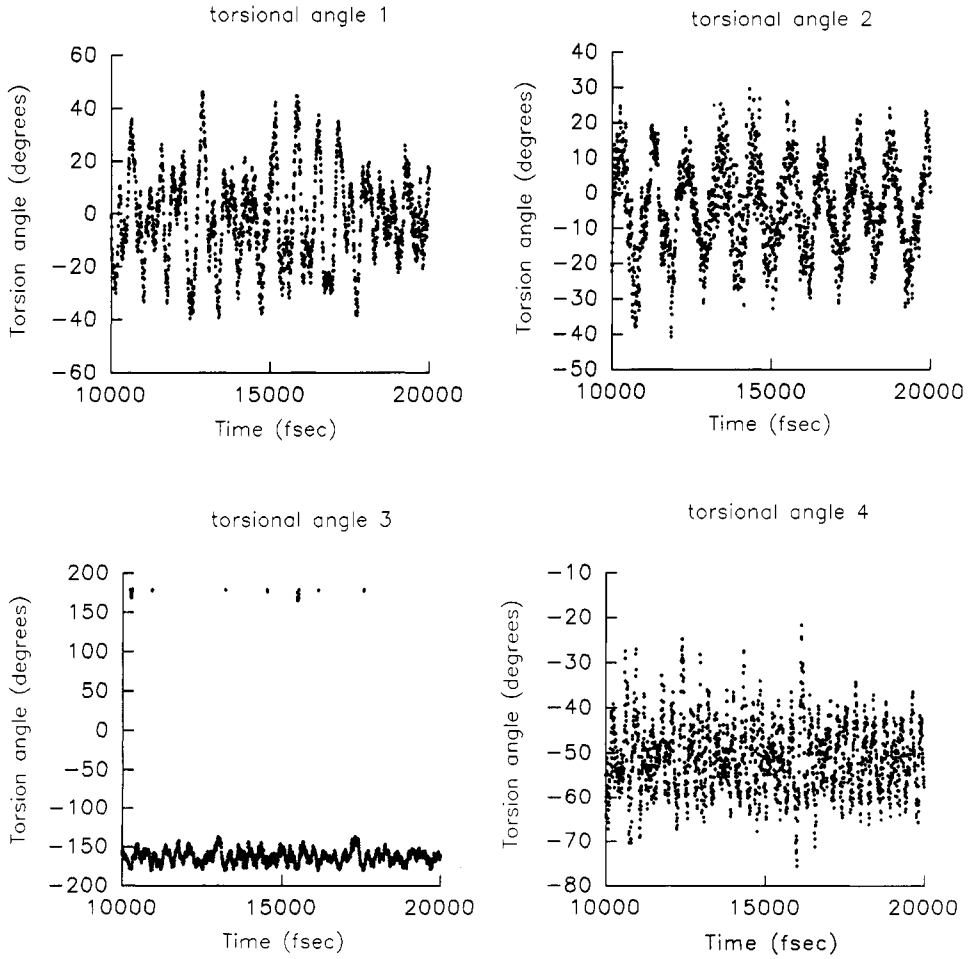

FIGURE 4: Torsion angle as a function of time. The molecule was equilibrated at 37 °C for 10 ps. Then the torsional angle was measured and plotted at 5-fs intervals. The average value and standard deviation of the torsional angle are shown in brackets in Table 2. The same data set is shown in Figure 3.

Table 2: Rotational Barriers of Selected Ryanodine Analogs[a]

compd	torsional angle no.	rotational minima (deg)	rel energy (kcal/mol)	rotational maxima (deg)	energy barrier (kcal/mol)
ryanodine	1	0	0		
				88	6
		180	0		
				186	7
		0	0		
		(359)			
		[358 ± 17]			
	2	192	10		
				267	17
		356	0		
				91	22
		192	10		
		(356)			
		[352 ± 19]			
	3[b,c]	73	19		
				150	33
		193	0		
				15	32
		73	19		
		(194.5)			
		[196 ± 7]			
	4	57	5		
				124	15
		188	2		
				229	8
		309	0		
				357	10
		57	5		
		(308.5)			
		[309 ± 7]			
		{68}			
anhydroester A	1	178	0		
				270	6
		358	0		
				90	6
		178	0		
		(0)			
		[358 ± 17]			
	2[b,c]	194	9		
				222	14.5
		357	0		
				84	22.5
		194	9		
		(357)			
		[353 ± 12]			
	3[c]	37	17		
				59	17
		73	17		
				152	27
		191	0		
				348	28
		37	17		
		(191)			
		[196 ± 6]			
	4	100	0		
				199	7
		279	2		
				298	3
		316	2		
		100	0	9	8
		(99)			
		[107 ± 24]			
		{342.5}			

[a] The numbers in parentheses are the torsional angles found at the global minimum of each molecule. They are the *anti* conformer unless otherwise indicated. The relative energy is arbitrarily set to zero for the lowest energy conformer (which has the same energy—within 1 kcal—as the global minimum). The numbers in brackets are the average values and standard deviations of the torsional angles as described in Figure 4. As a convenience to the reader, the numbers in braces are the torsional angles at the energy minimum defined using the hydrogen at position 13 rather than atom 18. The energy barriers are relative to the energy of the lowest energy conformer and represent the barrier encountered starting from the global minimum and going from low to high values of torsional angle. All energies include the electrostatic contribution and have been rounded to the nearest kilocalorie. [b] The method of steepest descents was used. [c] Rotations around this bond were highly strained and led to distorted geometries whose torsional angles could not be accurately evaluated. The locations of the maxima and minima are more subject to error than the other determinations.

pyrrole-2-carboxylate. The calculated difference in the heat of formation of the *anti* and *syn* conformers of ryanodine is 2.8 kcal/mol. In both cases the low-energy conformer has the same pyrrole–carbonyl orientation. As an aside, it is noted that, in addition to electronic interactions between the pyrrole dipole and the dipole of the adjacent carbonyl, interactions with the hydroxyl groups in the ryanoids may also contribute to the stabilization of one of the pyrrole rotomers (Figure 2). Recall that for the *anti* conformer the pyrrole nitrogen is directed to the same side of ryanodine as the large cluster of hydroxyl groups. Support for the choice of the *anti* conformation also comes from NMR solution studies of ryanodine. The *anti* conformation assigned to ryanodine by molecular modeling techniques is in agreement with the experimental data of Jefferies *et al.* (1992).

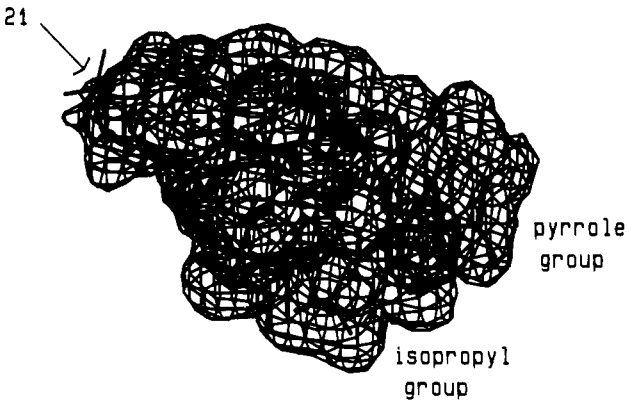

FIGURE 5: Miminum volume for ryanodine binding. The wire frame model is the intersection of the molecular volumes of all strongly binding ryanoids. Therefore, on the basis of the molecules tested, the wire frame represents the minimum molecular volume required for strong ryanodine binding. The location of some significant structural features is indicated by the labels.

(2) General Properties of Ryanoid Binding

In the next sections the general features of the ryanoids that correlate with strong binding to the skeletal muscle ryanodine receptor are examined by volume analysis and by CoMFA.

Correlation of Molecular Volumes and Binding. To visualize the regions of the ryanoids responsible for strong binding to the receptor, the intersections of the molecular volumes of tight-binding ryanoids [defined as those with dissociation constants (K_D) less than 100 nM] were computed (Figure 5). This figure presents the molecular volume common to all active analogs. The area enclosed by the wire frame can be interpreted as the minimum steric bulk required for strong binding, as judged for the compounds tested. Note that the methyl at position 21 is not essential for tight binding. The significance of this observation will be explored later when the interpretation of CoMFA is discussed.

To visualize the regions where steric bulk antagonizes ryanoid binding, two additional sets were derived: (1) the union of the molecular volumes of all weakly binding analogs ($K_D > 250$ nM) and (2) the union of tightly binding analogs ($K_D < 100$ nM) of ryanodine. The difference between these sets is illustrated in Figure 6. These volume elements are those found in one or more of the weakly binding compounds but not in any of the active analogs and represent steric bulk associated with loss of activity. Note that the volume near atoms 9 and 10 does not seem to correlate with loss of binding. This observation was made earlier on a smaller set of molecules and led the synthesis of the series of compounds with bulky substituents in this area [for example, the 10-equatorial substituents reported by Gerzon *et al.* (1993) and the 21-BODIPY-ryanodine reported here].

General Results of the CoMFA. To correlate molecular structure quantitatively with ryanoid binding to the skeletal muscle ryanodine receptor, a CoMFA was conducted (Cramer *et al.*, 1988). The results ($r^2 = 0.92$) were examined for those regions of the steric (Lennard-Jones) and electrostatic (Coulombic) fields most strongly correlated with the experimentally determined dissociation constants. The data are summarized in Figures 7–10 with an all-atom line drawing of ryanodine

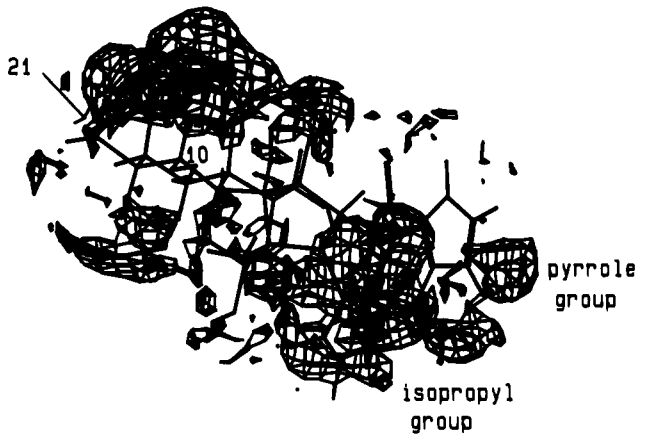

FIGURE 6: Steric inhibition of ryanodine binding. The wire frame model is the difference between the union of the molecular volumes of all weakly binding ryanoids and the union of the molecular volumes of all strongly binding ryanoids. The wire frame therefore represents those areas of excess steric bulk in poorly binding ryanoids. A stick model of ryanodine is shown for orientation.

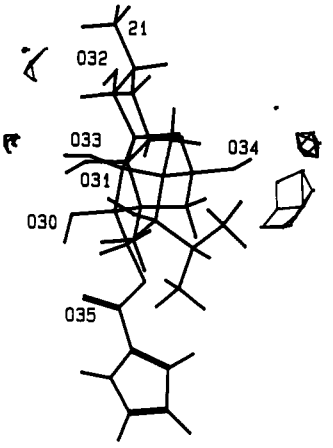

FIGURE 7: Correlation of electrostatic potential and binding. The wire frame is the result of a CoMFA and indicates the areas in which increasing negative charge is correlated with decreased binding. The wire frame contours connect points of half-maximal significance. A stick model of ryanodine is shown for orientation.

superimposed in the same orientation as the field contours. The wire frames represent the CoMFA output field of standard deviation times coefficient. The field was contoured at half-maximal value to localize those regions of the ryanoids most strongly correlated with binding.

The interactions between ryanoid and receptor can be divided into electrostatic and steric components. The CoMFA indicates they are of comparable importance in ryanoid binding. The electrostatic interactions (Figures 7 and 8) will be examined first. The wire frames in Figure 7 illustrate the two regions in which increasing negative charge is strongly associated with decreased strength of ligand binding. Both are located on hydroxyl groups. The largest area is centered on oxygen atom 34. This hydroxyl group is remote from the cluster of other hydroxyl groups (Figure 2). The smaller wire frames are centered on the cluster of hydroxyl groups (see Figures 1 and 2) including oxygen atoms 32 and 33. There is a strong correlation between increasing positive charge and decreased ligand affinity located in the broad bay between atoms 8 and 21 (Figure 8). Smaller areas of important electrostatic interaction are located in the cluster of hydroxyl groups and at the carbonyl oxygen of the pyrrole carboxylate.

The complex relationship between steric bulk and binding is diagramed in Figures 9 and 10. Increased steric bulk in

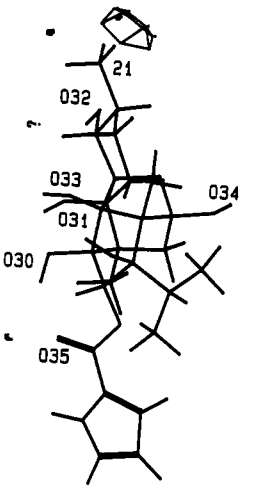

FIGURE 8: Correlation of electrostatic potential and binding. The wire frame is the result of a CoMFA and indicates the areas in which increasing positive charge is correlated with decreased binding. The wire frame contours connect points of half-maximal significance. A stick model of ryanodine is shown for orientation.

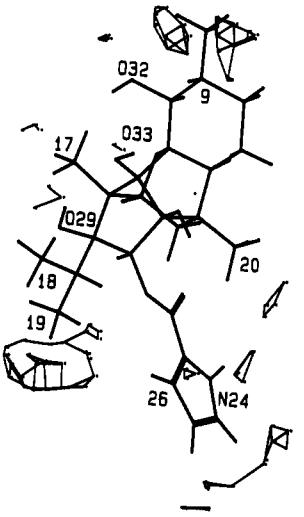

FIGURE 9: Correlation of steric bulk and binding. The wire frame is the result of a CoMFA and indicates the areas in which increasing steric bulk is correlated with increased binding. The wire frame contours connect points of half-maximal significance. A stick model of ryanodine is shown for orientation.

certain regions enhances ryanoid binding (Figure 9). The location of these regions is consistent with the molecular volume calculations described above. Importantly, the CoMFA indicates the strongest relationships are confined to three major loci: pyrrole, isopropyl, and position 9. Note that the strong correlation is for limited areas of the pyrrole and isopropyl groups rather than encompassing the entire region. The area around the nitrogen edge of the pyrrole group (N24 in Figure 1), the surface of the methyl group of carbon 19, and a section of the bay between atom 19 of the isopropyl group and atom 26 of the pyrrole group are important for binding. The enhancement of binding by steric bulk in the vicinity of position 10 (O32 in Figure 9) predicted by this model is supported by the 10-equatorial ryanoids which have been synthesized (Gerzon *et al.*, 1993).

Steric bulk can also inhibit binding of the ryanoids. The two regions which have the strongest relationship between steric bulk and inhibition of binding are shown in Figure 10. There is a large region at the outer surface of the methyl group extending upward from position 9 (carbon 21; see Figure 1). The other area extends from the surface of the methyl

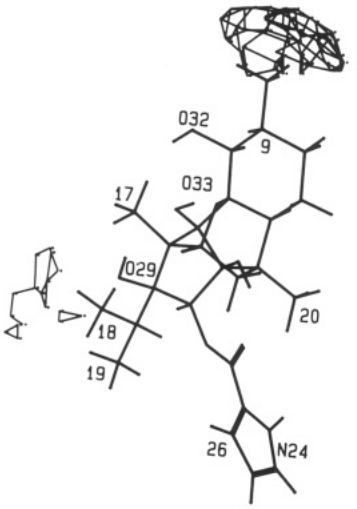

FIGURE 10: Correlation of steric bulk and binding. The wire frame is the result of a CoMFA and indicates the areas in which increasing steric bulk is correlated with decreased binding. The wire frame contours points of half-maximal significance. A stick model of ryanodine is shown for orientation.

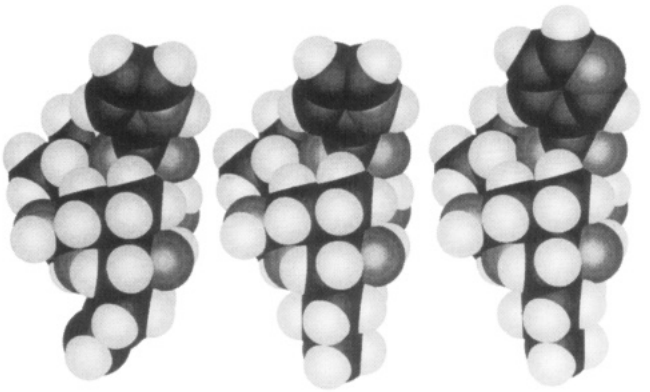

FIGURE 11: Comparison of the structures of ryanodine, dehydroryanodine, and ryanodyl nicotinate. To clearly illustrate the differences between these compounds, the structures of ryanodine (middle), dehydroryanodine (left), and ryanodyl nicotinate (right) are presented. The molecules were oriented by least-squares, rigid-body alignment of CoMFA fields.

group of carbon 19 into the space between the isopropyl group and the hydroxyl group of oxygen atom 29.

At first, the location of a region of strong correlation with binding near methyl carbon 21 seems to contradict the volume analysis which indicated that the methyl group was not important for binding. However, all additions to position 21 reduce binding somewhat (Scheme 1, Table 1). Therefore, this region will show a correlation with binding even though the site is not the primary locus of the ryanodine–receptor interaction. The point is important as one must understand the meaning of the CoMFA to correctly apply the results to ligand–receptor interactions. Consider dehydroryanodine and ryanodyl nicotinate (Figure 11). These two examples clearly demonstrate the greater importance of steric factors at the pyrrole nucleus relative to the methyl group at position 21. Dehydroryanodine binds with the same strength as ryanodine whereas the dissociation constant of ryanodyl nicotinate is 157-fold greater than that of ryanodine (Table 1). Small modifications located at opposite poles of the molecules have radically different effects on binding (Figure 11, Table 1). Note also that insertion of a bulky group such as BODIPY (**22**, Table 1) at the 21 position results in little perturbation of the dissociation constant. Together, these examples illustrate our claim that while alterations at position 21 correlate with binding, steric bulk at position 21 is of minor importance in determining the strength of binding.

Table 3: Contributions to Differences in Ryanoid Binding[a]

compd	(A) hydrophobic (kcal/mol)	(B) electrostatic (%)	(C) isopropyl (%)	(D) pyrrole (%)	(E) polycyclic ring (%)
ester A	−1.3–1.5	+63	−55	+4	−4
ester B	−2.5–2.6	−42	+32	−38	−10
ryanodyl nicotinate	−0.4–0.6	−46	−5	−33	−66
anhydroester A	+1.7–3.8	−29	−53	−1	−26
ryanodol	−2.1–2.2	−8	−15	−100	−11

[a] Predicted changes in binding are listed as kilocalories per mole for changes in hydrophobicity and as percent of difference between the natural logarithm of the dissociation constant of the listed compound and that of ryanodine. A plus (+) sign means that the change is predicted to enhance binding whereas a negative (−) sign indicated that the change is predicted to decrease binding. It is assumed for the purposes of this table that increases in hydrophobic energy increase binding strength. The compounds are arranged in order of increasing dissociation constant. The loss of binding energy is 1.7, 2.1, 3.1, 4.1, and 4.6 kcal/mol, respectively.

(3) Regional Assignments

Figures 7–10 localize the regions of the ryanoid molecule most strongly correlated with binding as deduced from the basis set. To augment the general picture, we have used the predict function of CoMFA to quantitatively estimate the contribution of specific attributes of an individual molecule to observed changes in binding affinity. Knowledge of the specific mechanism of the change in biological activity is useful in the design of new ligands. In Table 3 molecular attributes are grouped as (A) global hydrophobic interactions, (B) global electrostatic interactions, (C) all interactions at the isopropyl locus, (D) all interactions at the pyrrole locus, and (E) total polycyclic ring interactions. The last group (E) is defined as all interactions other than those with (1) the isopropyl and pyrrole groups and (2) any modified exocyclic atoms. Using ester A as an example, the interactions are those of all atoms except for the substituents at the 2, 3, 8, and 10 positions. For most ryanoids the last group (E) will quantitate the role of indirect effects. The point of this approach is to differentiate between those effects arising directly from the chemical modification at an exocyclic locus and those which arise from conformational alterations induced elsewhere in the molecule by the chemical modification. These regional assignments enhance the analysis of the binding data as illustrated below with a few examples.

First, consider the two global properties listed in Table 3, hydrophobicity and global electrostatic interactions. Neither appears to be correlated with the loss in binding energy (see legend of Table 3). Hydrophobic interactions are undoubtedly a significant factor in the binding of ryanoid to receptor, but the overall hydrophobicity (at least as measured by HINT) is an insufficient predictor of binding energy. The CoMFA model estimates that roughly one-half of the correlation between binding and structure is electrostatic (the other half is steric). As was the case with hydrophobicity, electrostatic interactions are undoubtedly a significant factor in the binding of ryanoid to receptor, but the global electrostatic interaction is an insufficient predictor of binding strength. Correlations between binding and physical properties such as hydrophobicity and electrostatics must be sought at specific loci as done by CoMFA.

Now consider the regional attributes (C, D, end E) of the ryanoids. Examination of Table 3 indicates that, in the case

of ryanodyl nicotinate, the obvious change at the pyrrole locus is important but the conformational changes in the ring system induced by the bulky group at the 3 position is an even stronger contributor to the observed loss of binding. In contrast, in the case of ryanodol essentially all of the loss of binding is due to the absence of the pyrrole group. In ester A relatively little of the loss in binding is due to changes in the polycyclic ring structure, but a large part of the difference is due to induced changes at the isopropyl locus. In contrast, in the case of ester B the modification produces induced changes at both the isopropyl and pyrrole locus, but these are offsetting. Only 10% of the loss in binding is due to the change in ring conformation resulting from the change in ring geometry at positions 9 and 10, and therefore this factor is not important in ryanodine binding. The analysis indicates that almost all of the loss of interaction energy is due to the direct interaction of the modified exocyclic groups at positions 8 and 10 with the receptor. Anhydroester A contains a major modification of the basic ryanoid ring structure, yet only about a quarter of the loss in binding is attributable to this feature. About one-half of the observed change is assigned to the change in position of the isopropyl group induced by the change in ring structure. The alteration in orientation of the isopropyl group is evident by comparing torsional angle 4 of ryanodine and anhydroester A (Table 2).

An important lesson gained from this analysis is that the obvious change in covalent structure may not be the primary cause of the alteration in biological properties. Induced changes secondary to the covalent modification may contribute much more to the change in the measured biological activity. Recognition and charting of these correlations provide a much more realistic view of the ligand–receptor interaction and facilitate the design of new analogs.

(4) Predicted Binding

The cross-validation and bootstrapping are statistical techniques used as part of the development of the CoMFA reported here. Both indicated the model was stable and was able to adequately predict the binding of a missing member of the basis set from the remaining members of the set. Nonetheless, it is more satisfying to predict the properties of compounds which are not members of the basis set. To demonstrate the predictive ability of the CoMFA, two compounds were chosen from the published literature. One is the 10_{eq}-CBZ-glycylryanodine synthesized by Gerzon *et al.* (1993). This compound presents a special challenge because of the large, floppy CBZ-glycyl pendent group. The experimental dissociation constant is 6.6 nM or essentially the same as reported here for the binding of ryanodine to rabbit skeletal muscle. The predicted dissociation constant varied from 7 to 14 nM. In general, those conformers with the pendent group extending away from the polycyclic ring system were predicted to bind better than those conformers where the CBZ-glycyl group was folded next to the polycyclic ring. Another test compound used was 18-hydroxyryanodine reported by Waterhouse *et al.* (1987). This compound is interesting because the CoMFA predicts that the isopropyl locus is particularly important in ryanoid binding: 18-hydroxyryanodine contains a polar group at this locus whereas all of the members of the basis set do not. From the reported data we estimate an experimental dissociation constant of 51 nM (IC_{50} = 88 nM) whereas the dissociation constant predicted by the present CoMFA is 19 nM. In both cases the CoMFA was able to predict another research group's data well, especially in light of the major departure in structure from the members of the basis set.

DISCUSSION

The purpose of this study was to define the regions of ryanodine critical to biological activity. In this paper structural properties of ryanodine and 18 analogs were correlated with the strength of interaction with the high-affinity site of the vertebrate skeletal muscle ryanodine receptor. The molecular volume calculation shows clearly that no steric bulk is required at the methyl (atom 21) position of ryanodine for activity (Figure 5). Increased steric bulk over wide regions of the ryanoids does not suppress binding (Figure 6); however, in other sections, notably in the isopropyl region, increased steric bulk decreases binding.

A CoMFA allowed us to quantitatively assess the contribution of particular parts of the ryanoid molecule to an observed biological effect—in this case binding to the skeletal muscle ryanodine receptor. The contours in Figures 7–10 were drawn at one-half of the maximum value so that only those areas which had the strongest correlation with binding are indicated. The interactions between the receptor and the isopropyl group and the pyrrole group are critical. Too much bulk in the pyrrole region (ryanodyl nicotinate) is as deleterious as lack of bulk (ryanodol). Areas associated with enhanced binding are located in close proximity to those regions associated with inhibition of binding (compare Figures 9 and 10). Therefore, conformational changes can markedly disrupt binding (*e.g.*, anhydroester A). Of the many hydroxyl groups, one appears to be particularly critical to ryanodine binding and is most likely the site of a hydrogen bond.

The volume difference maps (Figures 5 and 6) clearly show that the presence of the methyl group is not required for activity and that the region formed by atoms 9, 10, and 21 can tolerate large changes in structure without destroying binding (*e.g.*, BODIPY-ryanodine). Although the CoMFA shows that electrostatic and steric forces in this region strongly correlate with binding strength, the two observations are not contradictory as explained in the Results section. Alterations at the carbon-21 locus can modulate binding in two general ways: (1) by inducing conformational changes in remote regions of the molecule and (2) by weak interactions (either direct or via alterations in solvation) with amino acid residues on the surface of the receptor protein, near the entrance to the ryanodine binding site.

Interactions between the isopropyl and pyrrole loci are required to be precise since alterations in the conformation of these groups from the positions present in ryanodine markedly disrupt binding (*e.g.*, anhydroester A). A vital lesson emerged from the data: a visual inspection of the structure is likely to be misleading about the role a particular chemical modification plays in the observed biological activity. For example, in ryanodyl nicotinate over 60% of the net loss in binding energy (compared to ryanodine) arises from the change in the conformation of the basic, common structural backbone (Table 3). In many other cases a large part of the differences in dissociation constants result from conformation changes distributed throughout the molecules. Such insights would not be possible without CoMFA.

Binding of a ligand to a receptor is a combination of steric (see above) and electrostatic factors. The CoMFA indicates that, at least for this basis set, both contribute about equally to the statistical correlations between structure and affinity. The strongest correlations between electrostatic field and enhanced binding strength occurred near the hydroxyl groups

at the midpoint of the molecule. These are most probably sites for hydrogen bonding.

Based on the data as a whole, the following hypothesis about the ryanodine binding site is proposed. The pyrrole, isopropyl, and surrounding regions fit into a crevice on the receptor in a precise fit. Interactions include a strict van der Waals complementarity near the pyrrole and isopropyl groups as well as hydrogen bond interactions at the middle of the molecule. The methyl group (atom 21) and surrounding ring (especially atoms 9 and 10) are at the entrance of the binding pocket. These atoms are open to the solvent, and for that reason the interactions between ligand and receptor are relaxed. Nonetheless, the ryanoids can interact with amino, carboxyl, or other functional groups at the throat of the binding site. Interactions between this part of the ligand can modulate the strength of binding without being essential for the tight-binding process (compare changes at the two poles of the ryanoids). In this situation the electrostatic interactions are likely to be much more important than van der Waals interactions. Electrostatic interactions are nondirectional and have less dependence on distance than steric interactions (r *vs* r^6 and r^{12}). Hydrophobic interactions, which are also nondirectional, are also potentially important between substituents at the 21 position and the surrounding areas of the binding site. These interactions would be analogous to those underlying the enhancement of binding in affinity chromatography provided by the linker.

This preliminary study has identified regions of the ryanodine molecule important in binding to the receptor, and we have offered examples of the importance of these areas. Details of the interactions between ligand and receptor remain unknown, but our results indicate the direction of future studies to delineate the nature of the ryanodine receptor. Such experiments are underway. For example, ryanoids have been synthesized in which the pyrrolecarboxylic acid has been relocated or replaced with amino acid derivatives. The CoMFA model was able to predict the dissociation constants of these novel ryanoids (manuscript in preparation). The data presented suggest new modifications of the ryanodine structure to elucidate the minimal requirements for tight binding as well as the design of ryanodine analogs which are synthetically more accessible. We are also exploring the relation between molecular structure and the complex effects on calcium release described in the introduction. Important questions include (1) what regions of ryanodine affect the calcium channel conductance states and (2) do the regions important in binding have a direct effect on the calcium channel gating. It has been found that different ryanoids induce subconductance states of the ryanodine receptor calcium channel with different amplitudes (Tinker *et al.*, 1994). A recent report (Humerickhouse *et al.*, 1993) indicates the existence of differential biological effects among the ryanoids. The results we obtain will aid in the search for useful pharmacological agents as well as endogenous factors which modulate the ryanodine receptor.

ACKNOWLEDGMENT

The authors thank Molecular Probes Inc. for generously making the fluorophore BODIPY available for these studies.

SUPPLEMENTARY MATERIAL AVAILABLE

An expanded version of Table 2 listing the results with additional ryanoids described in this paper (17 pages). Ordering information is given on any current masthead page.

REFERENCES

Airey, J. A., Beck, C. F., Murakami, K., Tanksley, S. J., Deerinck, T. J., Ellisman, M. H., & Sutko, J. L. (1990) *J. Biol. Chem. 265*, 14187–14194.

Allen, M. S., Tan, Y., Trudell, M. L., Narayanan, K., Schindler, L. R., Martin, M. J., Schultz, C., Hagen, T. J., Koehler, K., Codding, P. W., Skolnick, R., & Cook, J. M. (1990) *J. Med. Chem. 33*, 2343–2357.

Burkert, U., & Allinger, N. L. (1982) *Molecular Mechanics*, ACS Monograph 177, American Chemical Society, Washington, DC.

Campbell, K. P., Knudson, C. M., Imagawa, T., Leung, A. T., Sutko, J. L., Kahl, S. D., Raab, C. R., & Madson, L. (1987) *J. Biol. Chem. 262*, 6460–6463.

Carroll, F. I., Gao, Y., Rahman, M. A., Abraham, P., Parham, K., Lewin, A. H., Boja, J. W., & Kuhar, M. J. (1991a) *J. Med. Chem. 34*, 2719–2725.

Carroll, S., Skarmeta, J. G., Yu, X., Collins, K. D., & Inesi, G. (1991b) *Arch. Biochem. Biophys. 290*, 239–247.

Chu, A., Diaz-Munoz, M., Hawkes, M. J., Brush, K., & Hamilton, S. L. (1990) *Mol. Pharmacol. 37*, 735–741.

Clark, M. (1990) *Tetrahedron Comput. Methodol. 3*, 47–59.

Cramer, R. D., III, Patterson, D. E., & Bunce, J. D. (1988) *J. Am. Chem. Soc. 110*, 5959–5967.

DeVault, G. (1983) *New Farm*, 25–27 (May/June).

Fairhurst, A. S. (1971) *J. Labelled Compd. Radiopharm. 7*, 133–136.

Fairhurst, A. S. (1974) *Am. J. Physiol. 227*, 1124–1131.

Fairhurst, A., & Hasselbach, W. (1970) *Eur. J. Biochem. 13*, 504–509.

Fleischer, S., Ogunbunmi, E. M., Dixon, M. C., & Fleer, E. A. M. (1985) *Proc. Natl. Acad. Sci. U.S. A. 82*, 7256–7259.

Frank, M., & Sleator, W. W. (1975) *Naunyn-Schmeideberg's Arch. Pharmacol. 290*, 35–47.

Gasteiger, J., & Marsili, M. (1980) *Tetrahedron 36*, 3219–3228.

Gasteiger, J., & Marsili, M. (1981) *Org. Magn. Reson. 15*, 353–360.

Gerzon, K., Humerickhouse, R. A., Besch, H. R., Jr., Bidasee, K. R., Emmick, J. T., Tian, Z., Ruest, L., & Sutko, J. L. (1993) *J. Med. Chem. 36*, 1319–1323.

Hansch, C., & Leo, A. (1979) *Substituent Constants for Correlation Analysis in Chemistry and Biology*, J. Wiley and Sons, New York.

Hilgemann, D. W., Delay, M. J., & Langer, G. A. (1983) *Circ. Res. 53*, 779–793.

Hillyard, I. W., & Procita, L. (1959) *J. Pharmacol. Exp. Ther. 127*, 22–28.

Homans, S. W. (1990) *Biochemistry 29*, 9110–9118.

Humerickhouse, R., Besch, H. R., Jr., Gerzon, K., Ruest, L., Sutko, J. L., & Emmick, J. T. (1993) *Mol. Pharmacol. 44*, 412–421.

Inui, M., Saito, A., & Fleischer, S. (1987) *J. Biol. Chem. 262*, 1740–1747.

Jefferies, P. R., Lam, W.-W., Toia, R. F., & Casida, J. E. (1992) *J. Agric. Food Chem. 40*, 509–512.

Jefferies, P. R., Lehmberg, E., Lam, W.-W., & Casida, J. E. (1993) *J. Med. Chem. 36*, 1128–1135.

Jenden, D. J., & Fairhurst, A. S. (1969) *Pharmacol. Rev. 21*, 1–25.

Jones, L. R., & Cala, S. E. (1981) *J. Biol. Chem. 256*, 11809–11818.

Jones, L. R., Besch, H. R., Jr., Sutko, J. L., & Willerson, J. T. (1979) *J. Pharmacol. Exp. Ther. 209*, 48–55.

Kauzmann, W. (1959) *Adv. Protein Chem. 14*, 1–63.

Kaye, P. T., Macrae, R., Meakins, G. D., & Patterson, C. H. (1980) *J. Chem. Soc., Perkin Trans. 2*, 1631–1635.

Kellogg, G. E., Semus, S. F., & Abraham, D. J. (1991) *J. Comput.-Aided Mol. Des. 5*, 545–552.

Kim, K. H., & Martin, Y. (1991a) *J. Org. Chem. 56*, 2723–2729.

Kim, K. H., & Martin, Y. C. (1991b) *J. Med. Chem. 34*, 2056–2060.
Lai, F. A., Erickson, H. P., Rousseau, E., Liu, Q.-Y., & Meissner, G. (1988) *Nature 331*, 315–319.
Lai, F. A., Misra, M., Xu, L., Smith, H. A., & Meissner, G. (1989) *J. Biol. Chem. 264*, 16776–16785.
Lattanzio, F. A., Jr., Schlatterer, R. G., Nicar, M., Campbell, K. P., & Sutko, J. L. (1987) *J. Biol. Chem. 262*, 2711–2718.
Liu, Q.-Y., Lai, F. A., Rousseau, E., Jones, R. V., & Meissner, G. (1989) *Biophys. J. 55*, 415–424.
Maret, G., El Tayar, N., Carrupt, P. A., Testa, B., Jenner, P., & Baird, M. (1990) *Biochem. Pharmacol. 40*, 783–792.
Marshall, G. R., & Cramer, R. D., III (1988) *Trends Pharmacol. Sci. 9*, 285–289.
Marsili, M., & Gasteiger, J. (1980) *Croat. Chem. Acta 53*, 601–614.
Meissner, G. (1986) *J. Biol. Chem. 261*, 6300–6306.
Nakai, J., Imagawa, T., Hakamata, Y., Shigekawa, M., Takeshima, H., & Numa, S. (1990) *FEBS Lett. 271*, 169–177.
Nayler, W. G., Daile, P., Chipperfield, D., & Gan, K. (1970) *Am. J. Physiol. 219*, 1620–1626.
Nozaki, Y., & Tanford, C. (1971) *J. Biol. Chem. 246*, 2211–2217.
Otsu, K., Willard, H. F., Khanna, V. K., Zorzato, F., Green, N. M., & MacLennan, D. H. (1990) *J. Biol. Chem. 265*, 13472–13483.
Penefsky, Z. J. (1974) *Pfluegers Arch. 347*, 173–184.
Penefsky, Z. J., & Kahn, M. (1970) *Am. J. Physiol. 218*, 1682–1686.
Pessah, I. N., & Zimanyi, I. (1991) *Mol. Pharmacol. 39*, 679–689.
Pessah, I. N., Waterhouse, A. L., & Casida, J. E. (1985) *Biochem. Biophys. Res. Commun. 128*, 449–456.
Pessah, I. N., Francini, A. O., Scales, D. J., Waterhouse, A. L., & Casida, J. E. (1986) *J. Biol. Chem. 261*, 8643–8648.
Powell, M. J. D. (1977) *Math. Program. 12*, 241–254.
Press, W. H., Flannery, B. P., Teukolsky, S. A., & Vetterling, W. T. (1988) *Numerical Recipes in C, The Art of Scientific Computing*, pp 301–327, Cambridge University Press, Cambridge.
Rogers, E. F., Koniuszy, F. R., Shavel, J., Jr., & Folkers, K. (1948) *J. Am. Chem. Soc. 70*, 3086–3088.
Rousseau, E., Smith, J. S., & Meissner, G. (1987) *Am. J. Physiol. 253*, C364–C368.
Ruest, L., Taylor, D. R., & Deslongchamps, P. (1985) *Can. J. Chem. 63*, 2840–2843.
Silipo, C., & Vittoria, A., Eds. (1991) *Pharmacochemistry Library*, Vol. 16, Elsevier, Amsterdam.
Smith, J. S., Imagawa, T., Ma, J., Fill, M., Campbell, K. P., & Coronado, R. (1988) *J. Gen. Physiol. 92*, 1–26.
Sutko, J. L., Willerson, J. T., Templeton, G. H., Jones, L. R., & Besch, H. R., Jr. (1979) *J. Pharmacol. Exp. Ther. 209*, 37–47.
Sutko, J. L., Ito, K., & Kenyon, J. L. (1985) *Fed. Proc. 44*, 2984–2988.
Sutko, J. L., Thompson, L. J., Schlatterer, R. G., Lattanzio, F. A., Fairhurst, A. S., Campbell, C., Martin, S. F., Deslongchamps, P., Ruest, L., & Taylor, D. R. (1986) *J. Labelled Compd. Radiopharm. 23*, 215–222.
Takeshima, H., Nishimura, S., Matsumoto, T., Ishida, H., Kangawa, K., Minamino, N., Matsuo, H., Ueda, M., Hanaoka, M., Hirose, T., & Numa, S. (1989) *Nature 339*, 439–445.
Tinker, A., Sutko, J. L., Ruest, L., Welch, W., Airey, J. A., Gerzon, K., Bidasee, K., Besch, H. R., Jr., & Williams, A. J. (1994) *Biophys. J. 66*, A315.
Waterhouse, A. L., Holden, I., & Casida, J. E. (1984) *J. Chem. Soc., Chem. Commun. 118*, 1265–1266.
Waterhouse, A. L., Pessah, I. N., Francini, A. O., & Casida, J. E. (1987) *J. Med. Chem. 30*, 710–716.
Zorzato, F., Fujii, J., Otsu, K., Phillips, M., Green, M. N., Lai, F. A., Meissner, G., & MacLennan, D. H. (1990) *J. Biol. Chem. 265*, 2244–2256.